



Published in final edited form as:

*Angle Orthod.* 2015 January ; 85(1): 18–25. doi:10.2319/011314-45.1.

## Three-dimensional canine displacement patterns in response to translation and controlled tipping retraction strategies

Shuning Li<sup>a</sup>, Zeyang Xia<sup>b</sup>, Sean Shih-Yao Liu<sup>c</sup>, George Eckert<sup>d</sup>, and Jie Chen<sup>e</sup>

<sup>a</sup>Postdoctoral Fellow, Department of Mechanical Engineering, Indiana University Purdue University Indianapolis, Indianapolis, Ind.

<sup>b</sup>Associate Professor, Shenzhen Institutes of Advanced Technology, Chinese Academy of Sciences and The Chinese University of Hong Kong, China

<sup>c</sup>Assistant Professor, Department of Orthodontics and Oral Facial Genetics, School of Dentistry, Indiana University, Indianapolis, Ind.

<sup>d</sup>Biostatistician Supervisor, Department of Biostatistics, Indiana University School of Medicine, Indianapolis, Ind.

<sup>e</sup>Professor and Chair, Department of Mechanical Engineering, and Professor, Department of Oral Facial Development, Indiana University Purdue University Indianapolis, Indianapolis, Ind.

### Abstract

**Objective**—To validate whether applying a well-defined initial three-dimensional (3D) load can create consistently expected tooth movement in patients.

**Materials and Methods**—Twenty-one patients who needed bilateral canine retraction to close extraction space were selected for this split-mouth clinical trial. After initial alignment and leveling, two canines in each patient were randomly assigned to receive either translation (TR) or controlled tipping (CT) load. The load was delivered by segmental T-loops designed to give specific initial moment/force ratios to the canines in each treatment interval (TI), verified with an orthodontic force tester. Maxillary dental casts were made before canine retraction and after each TI. The casts were digitized with a 3D laser scanner. The digital models were superimposed on the palatal rugae region. The 3D canine displacements and the displacement patterns in terms of TR, CT, and torque were calculated for each TI.

**Results**—The method can reliably detect a TR displacement greater than 0.3 mm and a rotation greater than 1.5°. Ninety-two TIs had displacements that were greater than 0.3 mm and were used for further analysis. Most displacements were oriented within  $\pm 45^\circ$  from the distal direction. The displacement pattern in terms of TR or CT was not uniquely controlled by the initial moment/force ratio.

**Conclusions**—The initial load system is not the only key factor controlling tooth movement. Using a segmental T-loop with a well-controlled load system, large variations in canine displacement can be expected clinically.

### Keywords

Orthodontic tooth movement; Translation; Controlled tipping

---

## INTRODUCTION

Orthodontic tooth movement is triggered by a load system consisting of six force and moment components delivered by orthodontic appliances. Tooth movement can be described by different displacement patterns such as controlled tipping (CT), translation (TR), or root torque. It is believed that the given initial load system with certain moment/force ratios (M/F) can control displacement patterns.<sup>1,2</sup> However, this theory has not been clinically validated.

Validation requires precise control of the three-dimensional (3D) initial load system and the ability to quantify the 3D tooth displacement clinically. Traditionally, the clinical tooth displacement was quantified by using two-dimensional (2D) cephalometric analysis,<sup>3-7</sup> which is incapable of detecting tooth displacement in the directions perpendicular to the sagittal plane.<sup>3,8</sup> Clinical 3D displacements can be calculated from digital models reconstructed from cone-beam computed tomography images<sup>9</sup> and digitized dental casts.<sup>10-14</sup>

The 3D displacement analysis commonly requires overlapping before and after treatment digital models and calculation of tooth displacement between the models.<sup>11-13</sup> The major challenge is to define a stable region or landmarks for model registration during an overlapping process. Previous studies have used a midpalatal orthodontic implant,<sup>13</sup> palatal rugae,<sup>11</sup> or four landmarks on the casts.<sup>12</sup> Insertion of implants is invasive, and the accuracy of the calculated rotation is largely reduced because of the previous ways of selecting the registration points.

The objectives of this study were (1) to develop a method to quantify the clinical 3D canine displacements and (2) to investigate whether initial loads (moment and force) of segmental T-loops can well control the tooth displacement patterns. Two canines of the same patient were retracted by two treatment strategies, TR or CT. The designated tooth movement (TR or CT) was implemented by using segmental T-loops with differential M/F.<sup>15</sup> We hypothesized that the canine displacement pattern is uniquely controlled by the initial load system, particularly differential M/F.

## MATERIALS AND METHODS

Twenty-one patients (9 men and 12 women) participated in this split-mouth trial study at the Indiana University School of Dentistry orthodontic clinic. The study was approved by Indiana University's Institutional Review Board. The average age of the patients was 21 years. These patients needed bilateral maxillary canine retractions (symmetrical pattern)

after the upper dental arches were bracketed, leveled, and aligned with sequential archwires to close the first premolar extraction spaces as parts of their treatment plans. Patients should have typical radiographically identified dental anatomy (average root sizes, bone insertion, and shape). No palatal expansion was needed during the treatment. All patients were allocated into two groups using the fixed allocation randomization method. Therefore, equal numbers of the canines were treated under either the CT or TR strategy.

The CT and TR strategies were accomplished by using specifically designed segmental T-loops (Figure 1).<sup>1,15</sup> The load system was individually validated for each canine using an orthodontic load tester. The initial load system in this study consisted of a distal retraction force of  $124.4 \pm 3.3$  cN along the maxillary arch, an anti-tipping and an anti-rotation moment along with minimized force and moment components in other directions. The details of the wire design and orthodontic force verification were reported previously.<sup>15</sup> The orthodontist who treated patients was provided with the readily made T-loops assigned to the canines and not informed of the patients' group affiliation. Patients were scheduled for a regular appointment every 5 to 6 weeks and normally underwent multiple treatment intervals (TIs). A TI was defined as when the interbracket distance between the canine and the second molar on one side reduced more than 1 mm. When a TI ended, a pair of new T-loops was redesigned consistent with the designated treatment strategies. Maxillary dental casts before the canine retraction and after each TI were made to record the tooth displacements. The study was completed when either the CT or TR side finished the canine retraction with the canine in the upright position judged by the clinicians using visual evaluation.

Each dental cast was scanned and digitized with an OPTIX 400S (3D Digital Corp, Sandy Hook, Conn) 3D laser scanner. The highest resolution (0.06 mm) was used to obtain the best representation of the cast surfaces. Seven to nine images of each cast taken from different directions were used to reconstruct the cast into a 3D digital model by using RapidForm (INUS Technology Inc, Seoul, South Korea).

For each canine, the origin of the coordinate system (CS) was set at the crown center, which was the bisection of the two interproximal contact points (Figure 2a). The x- and y-axes formed a plane that was parallel to the posterior occlusal plane. This plane was constructed by connecting the two second premolar buccal cusp tips and two first molar mesiobuccal cusp tips using the principal component analysis best-fitting method<sup>12</sup> (Figure 2b). For the CS on the left side, the positive x-axis is directed buccally, the y-axis distally, and the z-axis apically (Figure 3a). For the CS on the right side, the positive y-axis is directed mesially (Figure 3b). To be consistent, the displacement components on the right CS were converted to be expressed on the left CS.

Each TI had two digital models, pre-TI and post-TI. The two models were aligned by overlapping the 3D palatal (rugae) area, which was minimally changed during the treatment (highlighted area in Figure 4a).<sup>12,16</sup> The basis of the superimposition technique is a geometric optimization algorithm, iterative closest point.<sup>17</sup> Figure 4b shows the overlapped dental casts with the pre-TI model being coded in white and the post-TI model in black. Next, the crowns of the canine in the two superimposed models were aligned using the entire crown surface points for improving accuracy. The transformation matrix between the

two crown models was calculated. Then, the canine's six displacement components were computed from the entries of the transformation matrix<sup>9</sup> and translated into the clinically used terms. The process was repeated for each TI.

Mixed-model analysis of variance was used to compare the CT and TR strategies while accounting for the multiple TIs within each patient (significant at  $P < .05$ ).

The teeth displacement pattern was placed into three categories: CT, TR, and torque.<sup>7</sup> With the ability to quantify the tooth rotations, the pattern would be easily characterized by the tooth's mesial-distal crown-tipping angles,  $n^\circ$ . TR was defined when a canine was at the upright position within a range  $\pm n^\circ$ , CT was defined when the canine tipped distally more than  $n^\circ$ , and torque when the canine tipped mesially more than  $n^\circ$ . The definitions of CT, TR, and torque are shown in Table 1. The angles ( $n^\circ$ ) used for defining the ranges were chosen based the clinicians' ability to judge visually whether a tooth was in an upright position in the clinic. Two levels of definitions were used to differentiate the effects of the  $n^\circ$  selection on the outcomes.

The repeatability of model digitalization and reconstruction was evaluated by repeatedly scanning the same dental cast five times and assessing errors among these scans. Five different pairs of digital models from the five scans were selected. For each pair, one was set as pre-TI and the other was the post-TI model. The canine displacement in terms of its six translation and rotation components were calculated. Since the models were from the same cast, each pair should result in zero displacement, theoretically. The means and standard deviations of the displacements were determined, which represents the accuracy and variation levels.

## RESULTS

The averages of the translational and rotational components were calculated. The repeatability represented by the intraclass correlation coefficient was .9350 for translation and .9943 for rotation, indicating high consistency of displacement calculation. The maximum averaged displacement between paired pre-TI and post-TI models was 0.26 mm ( $\pm 0.06$  mm) for TR and  $1.33^\circ$  ( $\pm 0.08^\circ$ ) for rotation. These were considered as the noise level of the method.

Each patient experienced multiple TIs. The TIs with overall translation less than 0.3 mm (noise level) were excluded because the direction of tooth translation was uncertain. After excluding these TIs, 92 TIs remained (49 for CT and 43 for TR). The means and standard deviations of the canine displacement components are summarized in Tables 2 to 5. A 3D tooth displacement consists of three translational and three rotational components. Translational components on the CT side are shown in Table 2. Using the T-loops designed for CT, in the mesial-distal direction, the canines moved distally ( $1.0 \pm 0.5$  mm). In the buccal-lingual direction, the canines were moved more frequently to the buccal side ( $0.4 \pm 0.3$  mm) in 31 TIs than the lingual side ( $0.5 \pm 0.4$  mm) in 18 TIs. In the gingival-occlusal direction, the canines were intruded ( $0.3 \pm 0.3$  mm) in 25 TIs and extruded ( $0.5 \pm 0.6$  mm) in 24 TIs.

Rotational components on the CT side are shown in Table 3. In the distal-mesial direction, both distal and mesial crown tipping was observed. The number of TIs with distal crown tipping was greater than the number of TIs with mesial crown tipping (30 to 19). In the buccal-lingual direction, more lingual crown tipping than buccal was observed (30 to 19). For rotation, the number of TIs with mesial-out rotation was close to that of mesial-in rotations (26 to 23).

Translational components on the TR side are shown in Table 6. In the mesial-distal direction, 42 canines moved distally ( $1.0 \pm 0.5$  mm) and only 1 moved mesially. In the buccal-lingual direction, more TIs had lingual displacements ( $0.5 \pm 0.3$  mm) in 28 TIs than buccal displacement ( $0.4 \pm 0.2$  mm) in 15 TIs. In the gingival-occlusal direction, the canines were intruded ( $0.3 \pm 0.4$  mm) in 19 TIs and extruded ( $0.6 \pm 0.8$  mm) in 24 TIs.

Rotational components on the TR side are shown in Table 5. Among the rotation components, the number of TIs with distal crown tipping was slightly greater than the number of TIs with mesial crown tipping (22 to 21). The same observations could be found in the mesial-out/-in rotations (24 to 19). However, the difference in the number of TIs with lingual crown tipping and buccal crown tipping was more significant (18 to 25).

CT and TR strategies resulted in significantly different translational buccal-lingual direction displacements but did not create statistically significant differences in other translation and rotational displacements (Table 6). More CT-side TIs had buccal displacement (63.27%), and more TR-side TIs had lingual displacement (65.12%).

Under the controlled retraction load system, the canines moved generally distally. However, relatively larger lingual/buccal displacement components existed. Figure 5 shows that 41 of 49 TIs moved in the directions within  $45^\circ$  to distal direction on the CT side. Figure 6 shows that 36 of 43 TIs moved in the directions within  $45^\circ$  to the distal direction on the TR side.

Completion of the study was determined by the clinician based on completion of canine retraction on one of the two sides. Twenty of the 21 patients had CT-side spaces closed first. The mesial-distal crown-tipping angles for the 20 patients' last TIs are shown in Table 7. The CT-side canines were in the upright position with less than  $3^\circ$  mesial or distal crown tipping for all 20 patients.

The displacement patterns were obtained using the criteria defined in Table 1. Using  $2^\circ$  ( $n^\circ = 2^\circ$ ) as the criterion, the CT strategy resulted in 16 CT TIs (32.7%), 19 TR TIs (38.7%), and 14 torque TIs (28.6%); the TR strategy resulted in 12 CT TIs (27.9%), 18 TR TIs (41.9%), and 13 torque TIs (30.2%; Figure 7a). However, when using  $5^\circ$  ( $n^\circ = 5^\circ$ ) as a broader criterion, the CT strategy resulted in 4 CT TIs (8.2%), 44 TR TIs (89.8%), and 1 torque TI (2.0%); the TR strategy resulted in 5 CT TIs (11.6%), 36 TR TIs (83.7%), and 2 torque TIs (4.7%; Figure 7b).

## DISCUSSION

Currently, most clinical tooth displacements were reported in 2D and were measured between anatomical points.<sup>10-14</sup> These displacements were relative and did not include out-

of-plane components. The method developed for this study quantified the clinical 3D tooth displacement. The errors were 0.26 mm for translation and 1.33° for rotation. The error is smaller than that visually detectable clinically, thus improving the ability to quantify tooth displacement.

The displacement was reported with respect to the CS relative to the stale rugae region at the beginning of each TI, thus indicating absolute displacement. This displacement may not be intuitive clinically because canine displacement is commonly evaluated relative to the posterior segment, which may also move concomitantly (anchorage loss). Displacements reported in this study reflected the direct canine response to the applied load system expressed in the same CS. The magnitude of the tooth displacement was not the main focus of this study because the amount was dependent on the patient and affected by the treatment time, which varied significantly because of scheduling and missed appointments. For the purpose of this study, the displacement pattern, including tipping and translation as well as the movement direction, was of main interest.

When the CT strategy was used, it was expected that there should be a root correction at the end of the treatment. The root correction step was unnecessary in this study. All 21 CT cases ended up with the canines in the upright positions without using root-correction springs. There are two potential reasons. First, the force provided by the T-loop dropped faster than the moment, which led to an increase in M/F. With higher than the M/F for TR, the root would be tipped distally, similar to root correction in TR. Second, the crown of the tipping canine touched the crown of the second premolar first when the space was closed. In this situation, the second premolar provided a force to impede further canine crown tipping and made the canine return to the upright position.

According to our hypothesis, with a well-controlled initial load system, canine movement should be consistent. Our results failed to support the theory strongly. While the canines were retracted distally, they were also moved significantly in the buccal or lingual direction (Tables 2 and 4). Mesial canine displacement was noticed in only one TI, but it was 0.3 mm (close to error). With either 2° or 5° criteria, CT and TR strategies did not result in significantly different treatment outcomes (displacement patterns). The percentages of TIs that fell into each displacement pattern category were similar for both CT and TR strategies (Figure 7). The primary reason may be attributed to the behavior of the segmental T-loop. A previous study showed that the load system of the T-loop changed significantly as the canine moved.<sup>15</sup> The changes varied greatly among individuals, which may contribute to the large displacement pattern variation. In general, the M/F in the retraction direction increases as the canine is retracted. Because of the difficulty of controlling the tooth movement rate, the increase in M/F for each TI is different, causing the variation in displacement pattern. Other possible factors include (1) the alveolar bone quality, (2) the modeling and remodeling cycles, and (3) personal biological reaction to the load.

When segmental T-loops were used, the variation of the canine displacement components was large, although the initial load system was well controlled.<sup>15</sup> In orthodontic practice, the load system may not be as well controlled as reported in this study; thus, an even larger variation in canine movement may be expected. However, the results can be compared only

with tooth movement using segmental T-loops. A different level of variation is expected with other types of appliances.

## CONCLUSIONS

- The 3D method to quantify canine displacement can be used to quantify clinical 3D tooth displacement.
- The initial load system cannot uniquely determine the clinical tooth displacement when the segmental T-loop is used.

## ACKNOWLEDGEMENT

This research was supported by the NIH/NIDCR under grant #1R01DE018668.

## REFERENCES

1. Burstone CJ, Pryputniewicz RJ. Holographic determination of centers of rotation produced by orthodontic forces. *Am J Orthod.* 1980; 77:396–409. [PubMed: 6928741]
2. Gjessing P. Controlled retraction of maxillary incisors. *Am J Orthod Dentofacial Orthop.* 1992; 101:120–131. [PubMed: 1739066]
3. Hurst CA, Eppley BL, Havlik RJ, Sadove AM. Surgical cephalometrics: applications and developments. *Plast Reconstr Surg.* 2007; 120:92e–104e.
4. Downs WB. Analysis of the dentofacial profile. *Angle Orthod.* 1956; 26:191–212.
5. Steiner C. The use of cephalometrics as an aid to planning and assessing orthodontic treatment. *Am J Orthod.* 1960; 46:721–735.
6. Ricketts RM. Cephalometric analysis and synthesis. *Angle Orthod.* 1961; 31:141–156.
7. Proffit, WR.; Fields, HW.; Sarver, DM. *Contemporary Orthodontics.* 4th ed.. Mosby Elsevier; St Louis, Mo: 2007.
8. Lamichane M, Anderson NK, Rigali PH, Seldin EB, Will LA. Accuracy of reconstructed images from cone-beam computed tomography scans. *Am J Orthod Dentofacial Orthop.* 2009; 136:156 e1–6. [PubMed: 19651340]
9. Chen J, Li S, Fang S. Quantification of tooth displacement from cone-beam computed tomography images. *Am J Orthod Dentofacial Orthop.* 2009; 136:393–400. [PubMed: 19732674]
10. Commer P, Bourauel C, Maier K, Jager A. Construction and testing of a computer-based intraoral laser scanner for determining tooth positions. *Med Eng Phys.* 2000; 22:625–635. [PubMed: 11259931]
11. Keilig L, Piesche K, Jager A, Bourauel C. Applications of surface-surface matching algorithms for determination of orthodontic tooth movements. *Comput Methods Biomech Biomed Engin.* 2003; 6(5-6):353–359. [PubMed: 14675956]
12. Ashmore JL, Kurland BF, King GJ, Wheeler TT, Ghafari J, Ramsay DS. A 3-dimensional analysis of molar movement during headgear treatment. *Am J Orthod Dentofacial Orthop.* 2002; 121:18–29. [PubMed: 11786867]
13. Hayashi K, Uechi J, Murata M, Mizoguchi I. Comparison of maxillary canine retraction with sliding mechanics and a retraction spring: a three-dimensional analysis based on a midpalatal orthodontic implant. *Eur J Orthod.* 2004; 26:585–589. [PubMed: 15650067]
14. Cha BK, Lee JY, Jost-Brinkmann PG, Yoshida N. Analysis of tooth movement in extraction cases using three-dimensional reverse engineering technology. *Eur J Orthod.* 2007; 29:325–331. [PubMed: 17513876]
15. Xia Z, Chen J, Jiang F, Li S, Viecilli RF, Liu SY. Load system of segmental T-loops for canine retraction. *Am J Orthod Dentofacial Orthop.* 2013; 144:548–556. [PubMed: 24075663]
16. Hoggan BR, Sadowsky C. The use of palatal rugae for the assessment of anteroposterior tooth movements. *Am J Orthod Dentofacial Orthop.* 2001; 119:482–488. [PubMed: 11343019]

17. Besl PJ, McKay ND. A method for registration of 3-D shapes. *IEEE Trans Pattern Anal Machine Intell.* 1992; 14:239–256.



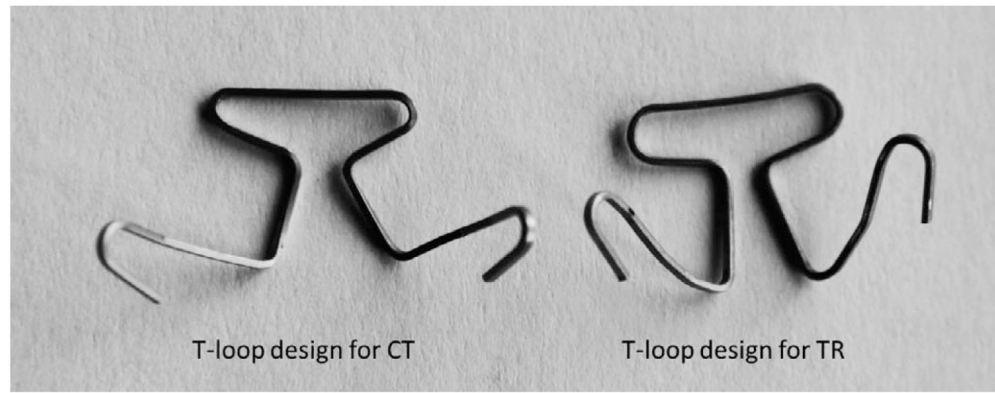


**Figure 1.** T-loop springs designed with the orthodontic load systems verified by an orthodontic load tester for either translation (TR) or controlled tipping (CT) strategy.

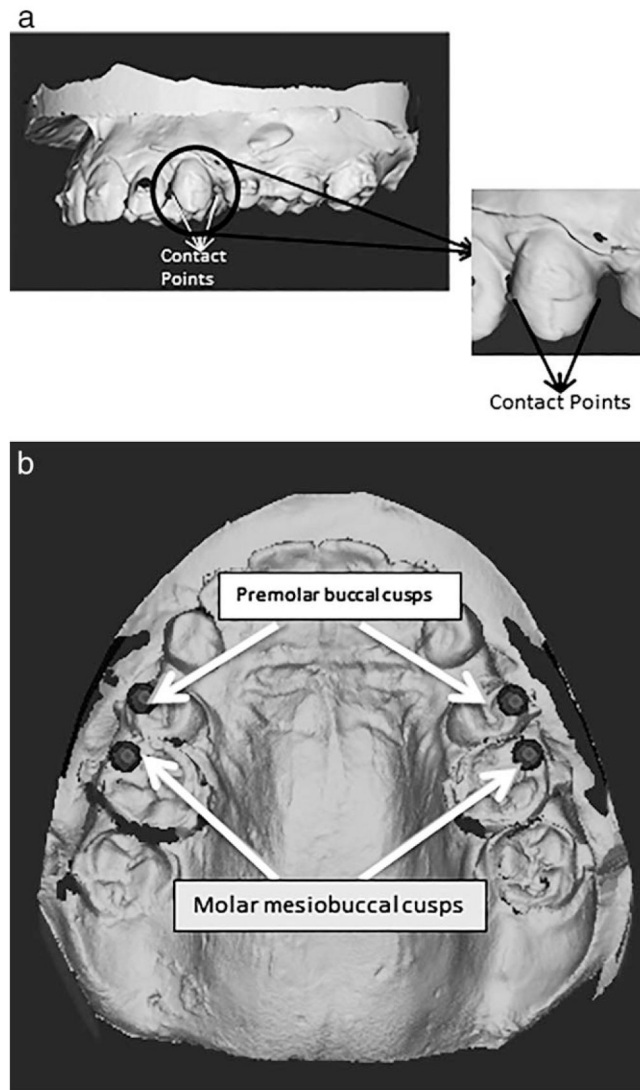


**Figure 2.** Landmarks to define the coordinate system. (a) The crown center located at the bisection of the two interproximate contact points for each canine. (b) The four points that define the occlusal plane.

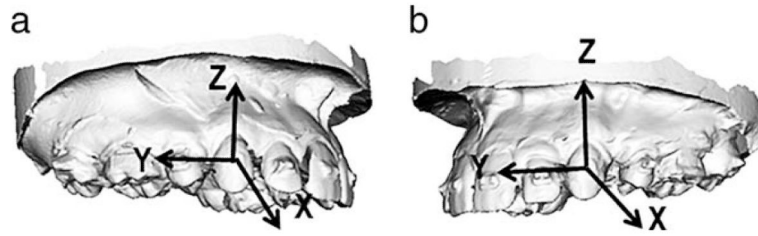


**Figure 3.**

(a) The coordinate system (CS) on the left canine with positive x in the buccal direction, positive y in the distal direction, and positive z in the apical direction. (b) The CS on the right canine with positive x in the buccal direction, positive y in the mesial direction, and positive z in the apical direction.

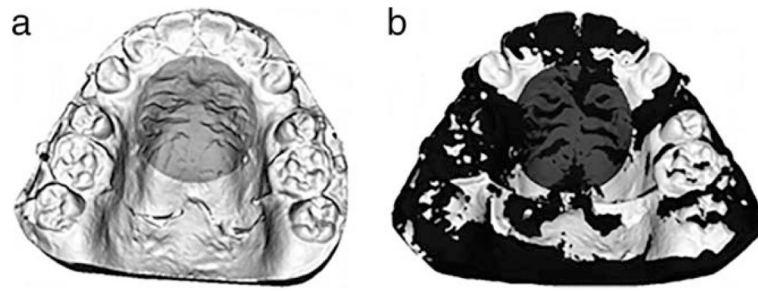


**Figure 4.** Superimposition of the pre-treatment interval (TI) and post-TI casts. (a) The highlighted region in the palatal area used for the superimposition. (b) The overlapped casts, with the pre-TI model coded white and the post-TI model black.

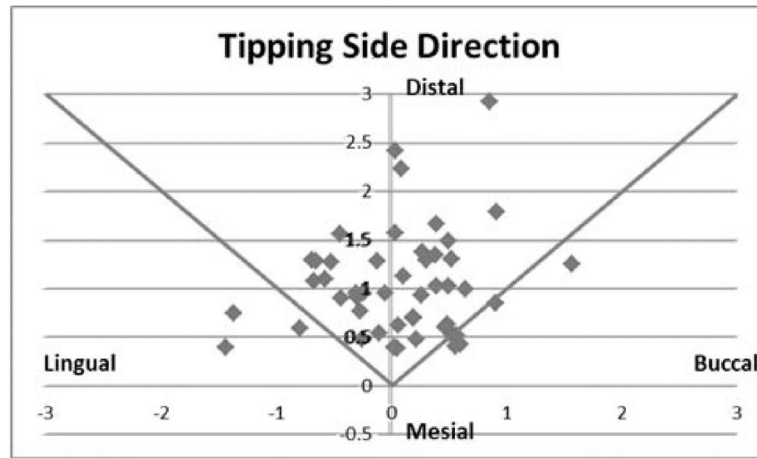


**Figure 5.** Canine displacements in the occlusal plane on the controlled tipping side.

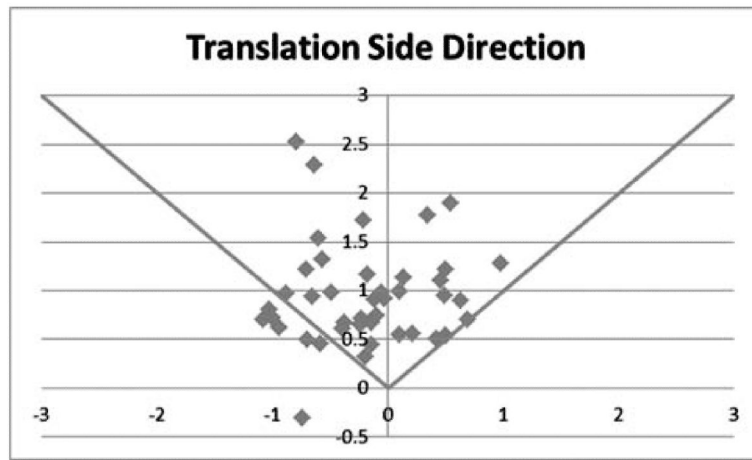


**Figure 6.** Canine displacements in the occlusal plane on the translation side.

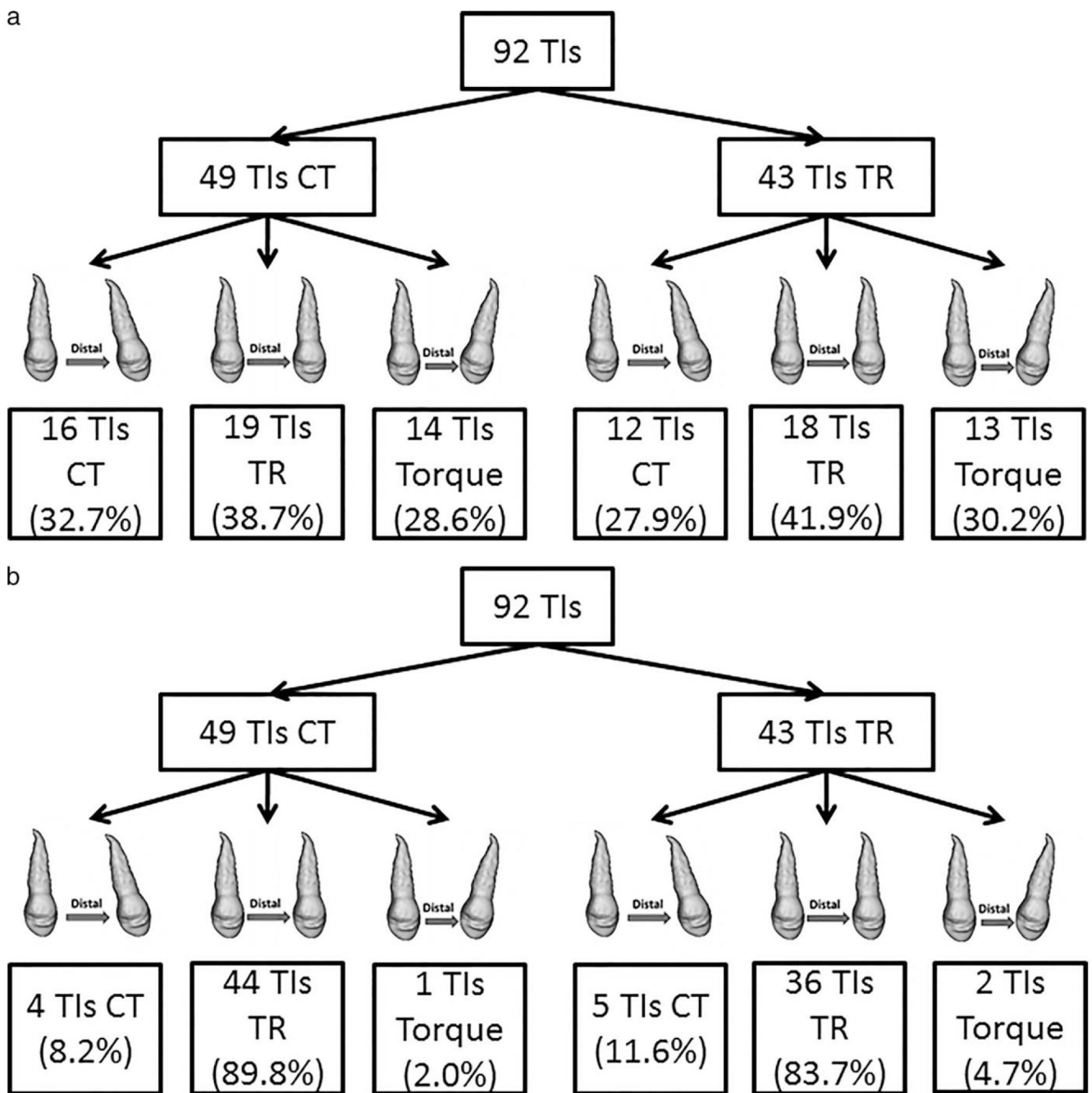


**Figure 7.** Canine displacement patterns resulting from either the controlled tipping or translation strategy using different translation definitions: (a) 2° criterion, (b) 5° criterion.

**Table 1**Canine Displacement Pattern Definition<sup>a</sup>

Controlled Tipping	Translation	Torque
> n° Distal crown tipping	n° Distal crown tipping or n° mesial crown tipping	>n° Mesial crown tipping

<sup>a</sup> n = the degree of mesial-distal crown-tipping angle.



**Table 2**

Translational Components (mm) in the Controlled Tipping Side

	<u>x-Axis</u>		<u>y-Axis</u>		<u>z-Axis</u>	
	<b>Buccal</b>	<b>Lingual</b>	<b>Distal</b>	<b>Mesial</b>	<b>Intrusion</b>	<b>Extrusion</b>
Number of treatment intervals	31	18	49	0	25	24
Minimum	0.0	0.0	0.4		0.0	0.0
Maximum	1.6	1.4	2.9		1.6	2.5
Average	0.4	0.5	1.0		0.3	0.5
Standard deviation	0.3	0.4	0.5		0.3	0.6

**Table 3**

Rotational Components (°) in the Controlled Tipping Side

	<b>x-Axis</b>		<b>y-Axis</b>		<b>z-Axis</b>	
	<b>Distal Crown Tipping</b>	<b>Mesial Crown Tipping</b>	<b>Lingual Crown Tipping</b>	<b>Buccal Crown Tipping</b>	<b>Mesial-Out Crown Rotation</b>	<b>Mesial-In Crown Rotation</b>
Number of treatment intervals	30	19	30	19	26	23
Minimum	0.0	0.2	0.1	0.1	0.1	0.2
Maximum	11.8	7.5	10.6	6.5	22.3	11.5
Average	3.2	2.7	3.3	2.6	2.9	2.9
Standard deviation	3.1	1.8	2.8	1.9	4.3	2.9

**Table 4**

Translational Components (mm) in the Translation Side

	<u>x-Axis</u>		<u>y-Axis</u>		<u>z-Axis</u>	
	<b>Buccal</b>	<b>Lingual</b>	<b>Distal</b>	<b>Mesial</b>	<b>Intrusion</b>	<b>Extrusion</b>
Number of treatment intervals	15	28	42	1	19	24
Minimum	0.1	0.0	0.3	0.3	0.0	0.0
Maximum	1.0	1.1	2.5	0.3	1.3	3.7
Average	0.4	0.5	1.0	0.3	0.3	0.6
Standard deviation	0.2	0.3	0.5		0.4	0.8

**Table 5**

Rotational Components (°) in the Translation Side

	<b>x-Axis</b>		<b>y-Axis</b>		<b>z-Axis</b>	
	<b>Distal Crown Tipping</b>	<b>Mesial Crown Tipping</b>	<b>Lingual Crown Tipping</b>	<b>Buccal Crown Tipping</b>	<b>Mesial-Out Crown Rotation</b>	<b>Mesial-In Crown Rotation</b>
Number of treatment intervals	22	21	18	25	24	19
Minimum	0.1	0.9	0.0	0.1	0.3	0.1
Maximum	13.5	9.2	7.6	7.8	13.9	10.7
Average	3.4	3.0	3.2	2.3	3.4	4.2
Standard deviation	3.1	2.5	2.5	1.9	3.5	3.2

**Table 6**Comparison Between Controlled Tipping and Translation-Side Displacement Components<sup>a</sup>

	<u>Translation</u>			<u>Rotation</u>		
	<u>x</u>	<u>y</u>	<u>z</u>	<u>x</u>	<u>y</u>	<u>z</u>
<i>P</i> value	.06	.47	.50	.70	.39	.50

<sup>a</sup>*P* < .05 = statistically significant.

**Table 7**

Controlled Tipping-Side Mesial-Distal Crown-Tipping Angles in Last Treatment Intervals (°)

Distal crown tipping	2.2	0.0	1.2	2.4	1.7	1.0	2.0	2.0	1.3
Mesial crown tipping	1.3	2.4	2.9	2.7	1.1	1.5	2.5	0.6	2.4
								0.6	0.0